Journal of Chromatography B, 1020 (2016) 53–61

Contents lists available at ScienceDirect

Journal of Chromatography B

journal homepage: www.elsevier.com/locate/chromb

Acute hydrodynamic damage induced by SPLITT fractionation and centrifugation in red blood cells

Adriana Urbina[a,b,*], Ruben Godoy-Silva[c], Mauricio Hoyos[d], Marcela Camacho[e,f]

[a] Universidad del Rosario, Biomedical Sciences Department, School of Medicine, Bogotá, DC, Colombia
[b] Universidad Nacional de Colombia, Bogotá, DC, Colombia
[c] Universidad Nacional de Colombia, Chemical and Environmental Engineering Department, Bogotá, DC, Colombia
[d] École Supérieure de Physique et Chimie Industrielles, Laboratoire de Physique et Mécanique des Milieux Hétérogènes (PMMH), UMR 7636CNRS, Paris, France
[e] Universidad Nacional de Colombia, Department of Biology, Bogotá DC, Colombia
[f] Centro Internacional de Física (CIF), Laboratorio de Biofísica, Bogotá, DC, Colombia

ARTICLE INFO

Article history:
Received 10 November 2015
Received in revised form 3 March 2016
Accepted 19 March 2016
Available online 22 March 2016

Keywords:
SPLITT fractionation
Centrifugation
Red blood cells
Hydrodynamic damage
Energy dissipation rate

ABSTRACT

Though blood bank processing traditionally employs centrifugation, new separation techniques may be appealing for large scale processes. Split-flow fractionation (SPLITT) is a family of techniques that separates in absence of labelling and uses very low flow rates and force fields, and is therefore expected to minimize cell damage. However, the hydrodynamic stress and possible consequent damaging effects of SPLITT fractionation have not been yet examined. The aim of this study was to investigate the hydrodynamic damage of SPLITT fractionation to human red blood cells, and to compare these effects with those induced by centrifugation. Peripheral whole blood samples were collected from healthy volunteers. Samples were diluted in a buffered saline solution, and were exposed to SPLITT fractionation (flow rates 1–10 ml/min) or centrifugation (100–1500 *g*) for 10 min. Cell viability, shape, diameter, mean corpuscular hemoglobin, and membrane potential were measured. Under the operating conditions employed, both SPLITT and centrifugation maintained cell viability above 98%, but resulted in significant sublethal damage, including echinocyte formation, decreased cell diameter, decreased mean corpuscular hemoglobin, and membrane hyperpolarization which was inhibited by EGTA. Wall shear stress and maximum energy dissipation rate showed significant correlation with lethal and sublethal damage. Our data do not support the assumption that SPLITT fractionation induces very low shear stress and is innocuous to cell function. Some changes in SPLITT channel design are suggested to minimize cell damage. Measurement of membrane potential and cell diameter could provide a new, reliable and convenient basis for evaluation of hydrodynamic effects on different cell models, allowing identification of optimal operating conditions on different scales.

1. Introduction

Obtaining red blood cell (RBC) fractions with high purity, yield, and viability is important for blood banks and transfusion medicine. Blood bank processing, which employs centrifugation, imposes mechanical forces on erythrocytes, which, as with any manufacturing process, may contribute to hemolysis and sublethal damage of the remaining cells, limiting their normal function and compromising their therapeutic effectiveness [1]. Split-flow fractionation (SPLITT) is a family of techniques that separates differently sized particles in thin, rectangular channels using gravitational and flow fields aligned perpendicularly to each other [2]. SPLITT fractionation allows continuous processing of whole blood without antibody labelling to obtain fractions of RBC, platelets and plasma proteins in short time with high purity and viability [3]. The absence of labelling and the use of very low flow rates and force fields are expected to induce very low shear stress and minimize cell damage, making it an attractive technique for large-scale separations [4].

RBCs, which in vivo are suspended cells that experience mechanical stress, have been recommended as a standard cell model for comparative assessment of the potential for damage in various hydrodynamic environments [5,6]. Since erythrocytes are

* Corresponding author at: Adriana Urbina, Universidad del Rosario, Biomedical Sciences Department, School of Medicine, Carrera 24 #63C-69, Bogotá, DC 111221, Colombia.
E-mail address: adriana.urbina@urosario.edu.co (A. Urbina).

http://dx.doi.org/10.1016/j.jchromb.2016.03.025
1570-0232/

enucleated post-mitotic cells and unable to multiply, the injurious effects of mechanical stress cannot be masked by the adaptive changes of cell growth and multiplication, as is observed in other cell types [7]. Additionally, red blood cell shape is extremely sensitive to metabolic and medium changes, and to mechanical stress [6]. Although it has been documented that different biomedical devices and bioreactors generate morphological changes in RBCs that are attributable to mechanical stress [8,5,9–11], the hydrodynamic stress and consequent damaging effects of SPLITT fractionation have not been yet determined, partly because it is assumed that the low flow rates and force fields used in this technique do not generate significant mechanical stress [12,4]. To test the apparent innocuousness of SPLITT separation, it is necessary to use very sensitive indicators for assessing cell damage. The aim of this study was to investigate the hydrodynamic damage of SPLITT fractionation on human red blood cells, and to compare these effects with those induced by centrifugation.

2. Materials and methods

2.1. Sample collection and preparation

This study was approved by the institutional Ethics Committee of the Universidad Nacional de Colombia and followed current protocols for research on humans and handling of biological samples (Declaration of Helsinki). Blood samples were collected in EDTA from healthy volunteers. Since the interactions between cells can generate changes in the flow profile in the SPLITT channel, it was necessary to prepare highly diluted cell suspensions (hematocrit 0.5%) using a saline solution containing (in mM): 140 NaCl; 5 KCl; 1$CaCl_2$; 1 $MgCl_2$; 10HEPES; 10 glucose; pH 7.4; 292 ± 1 mOsm/l; viscosity 0.00131 Pa·s; density 1007.1 kg/m^3 (chemicals were obtained from Sigma-Aldrich, St. Louis, MO, USA). This solution was used both for diluting samples and as a carrier fluid. The osmolarity of the solution was measured with a vapor pressure osmometer (Wescor Model 5600, ELITechGroup, Paris, France), the dynamic viscosity was measured with a cone and plate rheometer (Bohlin C-VOR 200, Malvern Instruments, Malvern, UK), and density was measured with a pycnometer. Since the use of plasma has been shown to be protective against mechanical damage in red blood cells [5], experiments with autologous plasma supplementation (final concentration of 10% v/v) were also conducted (311 ± 2 mOsm/l; 0.0016 Pa·s). Assays were performed at room temperature ($20 \pm 2\,^{\circ}C$).

2.2. SPLITT channel

A 186 mm long (L), 20 mm wide (B) and 0.48 mm deep (D) SPLITT channel was used. The channel was fabricated at the PMMH laboratory by alternating plates of Plexiglas (polymethyl methacrylate) and spacers of Mylar (polyethylene terephthalate) (Fig. 1A). The sample was injected through the inlet labelled *a* with a constant flow rate $Qa = 0.2$ ml/min, while the inlet *b* was fed with the carrier fluid at a variable flow rate Qb, so the total flow rate $Q = Qa + Qb = Qaí + Qbí$. In order to use the device in a hydrodynamic test to evaluate its maximal potential for damage, output fractions were collected only from the lower outlet labelled *b*, by keeping the outlet *a* closed. Total flow rates employed ranged from 1.5 to 10.0 ml/min, and were controlled with syringe pumps (Harvard Apparatus, Holliston, MA). Outlet fractions and non-treated controls were processed immediately for the measurement of morphological indicators and membrane potential.

2.3. Centrifugation

A bench centrifuge with a 45° fixed-angled rotor (Sorvall Biofuge Primo R, Thermo Scientific, Waltham, MA) was used to centrifuge 10 ml of cell suspension in polypropylene centrifuge tubes (Falcon™, BD Biosciences, San Jose, CA, USA) at $20 \pm 2\,^{\circ}C$ for 10 min at 100, 200, 400, 900 or 1500 g with no brake, equivalent to total centrifugal g-second values of 6, 12, 240, 540, or 900×10^4 g·s. respectively These centrifugation parameters are similar to those used in mononuclear blood cell isolation with Ficoll®-Paque and in blood bank processing [13].

2.4. Hemoglobin release

After one pass through the SPLITT channel, output fractions were collected and centrifuged at 2750g for 15 min at room temperature to obtain supernatants. In contrast, after centrifugation assays, supernatants were collected directly with no additional centrifugation. Supernatants thus obtained were frozen and stored at $-30\,^{\circ}C$ for subsequent analysis. Hemoglobin released in the supernatant was measured via optical absorbance at 414 nm using a microplate reader (Ultramark 550, Bio-Rad Laboratories, Hercules, CA, USA) with the Harboe method [14,15]. A calibration curve was constructed using a standard of 100% hemolysis by hypotonic lysis with distilled water and 12 1:2 serial dilutions until 0.024% hemolysis.

2.5. Cell morphology

Non-treated negative controls and output fractions were transferred into 24 well culture plates to obtain micrographs with an inverted light microscope (40× objective) equipped with an image acquisition system (AxioCam, Carl Zeiss MicroImaging, Göttingen, Germany). The captured images were stored in *.zvi* format and subsequently analyzed with the software AxioVision (SE64, Rel. 4.8; Carl Zeiss MicroImaging, Göttingen, Germany) to determine cell shape. Using the 40× dry objective, a portion of the image field was selected with no overlapping red blood cells, and 10 fields were counted using the zigzag method until completing 100 cells per experiment. The amount of echinocyte-discocyte transformation was determined by calculating the morphological index I Eq. (1), an indicator of extent of morphological change, by incorporating the classification of echinocytes from type I to III according to the number of spikes per cell [16]:

$$I = \lceil 1 \times \text{echinocytesI} \rceil + \lceil 2 \times \text{echinocytesII} \rceil + \lceil 3 \times \text{echinocytesIII} \rceil \quad (1)$$

Since the morphological index I increases with incubation time [17], a period of 2–3 h was standardized when performing the experiment.

2.6. Cell diameter

The cell diameter of one hundred cells per experiment (from 14 independent assays) was measured from photomicrographs by image analysis. At the beginning of each experiment, etched lines on a calibrated stage micrometer were used to set the μm/pixel conversion factor. Using the AxioVision image analysis software, a line was traced connecting the outer dark edges at the rims of each cell; only the horizontal diameter was measured for cells on edge, whereas for the cells lying flat the maximum diameter was recorded.

2.7. Mean corpuscular hemoglobin concentration

Total hemoglobin concentration (Hb; g/dl) was measured by the azide methemoglobin method, and hematocrit (Hct), by impedance cytometry using an automated haematological analyzer (Sysmex®

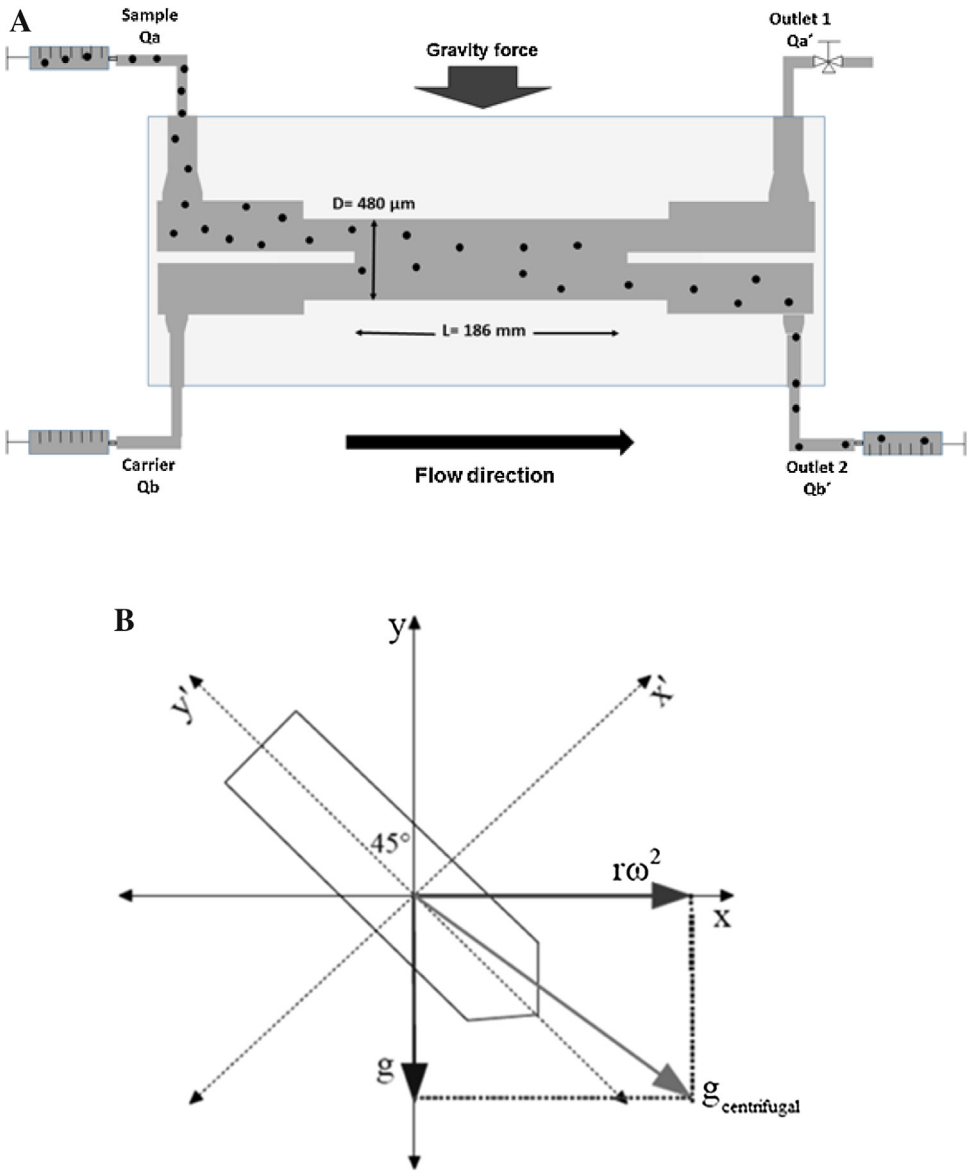

Fig. 1. Schematic view of the separation systems. (A) SPLITT channel; (B) geometric configuration of the centrifuge tube.

R480, Sysmex America Inc., Mundelein, IL, USA). Mean corpuscular hemoglobin concentration (MCHC) was calculated as the percentual relationship between total hemoglobin and hematocrit in the sample (MCHC = [Hb/Hct] × 100).

2.8. Computational fluid dynamic simulation

The flow through the SPLITT channel was simulated using the computational fluid dynamics software FLUENT® v14.0 (ANSYS, Canonsburg, PA, USA). The geometries of the SPLITT channel and the centrifuge tube were created using the program SOLIDWORKS® Standard (Dassault Systèmes SOLIDWORKS, Waltham, MA) and exported in *.igs* format. The complete SPLITT channel was modelled with a mesh optimization with a grid size of 7 µm at the inlets and outlets. For the centrifuge tube, the grid size was 9 µm at the bottom; for comparison purposes, the diameter of a RBC is 8.4 ± 0.6 µm. For the simulations in FLUENT, we used a pressure-based segregated method and a discrete phase model. No energy balance was imposed, as isothermal conditions and negligible friction losses were assumed. The implicit formulation was used to solve the equations for steady-state operation, assuming laminar flow and a viscous fluid model with absolute pressure of 74,660 Pa at the output (average atmospheric pressure at our laboratory). Boundary conditions included non-slip conditions at the walls and constant velocity at the inlets of the SPLITT channel. The schemes used for spatial discretization were: momentum, second order upwind; for pressure, the standard FLUENT interpolation; for gradient, least squares cell-based; and for pressure-velocity coupling, the SIMPLE scheme. Flow through the SPLITT channel was configured with two inlets (top for the sample and bottom for the carrier fluid) and one output (bottom). For the simulations of the centrifuge tube, we set an absolute pressure of 74,660 Pa, zero velocity at the center of the top, and gravity towards the bottom of the tube (Fig. 1B). All the simulations for the present study were performed using an Intel® CORE™ i7CPU running at 2.2 GHz with 6.0 GB RAM and 700 GB hard disk.

Fig. 1B shows the effect of earth gravitational and centrifugal fields (g and $r\omega^2$, respectively) on the centrifuge tube. The resultant vector g_c corresponds to the net acceleration acting on the tube. For the simulations, the Cartesian plane (xí, yí) was consid-

ered. The relative acceleration N generated by the rotor is defined by the relation between $r\omega^2$ and g Eq. (2):

$$N = \frac{r\omega^2}{g} \tag{2}$$

The components of the centrifugal acceleration vector g_c in the plane (x', y') are shown in Eq. (3):

$$g_{centrifugal} = \frac{\sqrt{2}}{2}\left(g(N-1); -g(N+1)\right) \tag{3}$$

At FLUENT convergence, residuals were 1×10^{-7}. An "execute on demand" user-defined function was implemented which calculated the energy dissipation rate (EDR) using the following equation [18]:

$$\varepsilon = \tau : \nabla\cup = \mu\left[\nabla\cup + (\nabla\cup)^T\right] : \nabla\cup$$
$$= \mu\sum_i\sum_j\left[\nabla\cup + (\nabla\cup)^T\right]_{ij}\nabla\cup_{ji} \tag{4}$$

where μ is the viscosity of the fluid, $\nabla\cup$ is the velocity gradient tensor, and $(\nabla\cup)^T$ is the transpose of $\nabla\cup$. EDR is a measure of the rate at which energy is drawn into the liquid, energy which is ultimately transformed into heat or absorbed by particles suspended in the fluid. EDR has units of energy density per unit time per unit volume (i.e., $J \cdot s^{-1} \cdot m^{-3}$), or power per unit volume (i.e., $W\,m^{-3}$).

2.9. Membrane potential

Resting membrane potential was determined by flow cytometry using the anionic voltage-sensitive fluorescent probe bis-(1,3-diethylthiobarbituric acid) trimethine oxonol ($DiSBAC_2(3)$; 568/590–630 nm; Thermo Fisher Scientific, Waltham, MA, USA). Samples were suspended in an external solution containing (in mM): 140 NaCl; 5 KCl; 1$CaCl_2$; 1 $MgCl_2$; 10HEPES; 10 glucose; pH 7.4; 310 mOsm/l (chemicals from Sigma-Aldrich). $DiSBAC_2(3)$ was used at a final concentration of 230 nM in the reaction mixture, which was incubated in the dark at room temperature ($20 \pm 2\,^{\circ}C$) for 30 min. For quantitative determination of the membrane potential, a calibration curve was constructed using valinomycin 1 μM (Thermo Fisher Scientific) and variable external potassium concentrations, after which the resting potential can be calculated as the Nernst potential for this ion [19]. For each run, unstained controls and a calibration curve were prepared. Fluorescence values were measured with a flow cytometer equipped with an argon ion laser (535/585 ± 62 nm) (FACSCanto II, BD Biosciences, San Jose, CA, USA). For each sample 100,000 events were acquired. Data were analyzed using the package Attune® Cytometric Software (v1.2.5; Thermo Fisher Scientific). The red blood cell population was selected from the light scatter cytogram (SSC vs. FSC), and membrane potential was calculated using the area under the curve (FL-1-A). When indicated, 2 mM ethylene-glycol-tetraacetic acid (EGTA) was used as Ca^{2+} buffer (Sigma-Aldrich). All solutions were filtered through 0.2 μm cellulose disks and equilibrated in air (oxygen partial pressure pO_2 = 117 mm Hg; carbon dioxide partial pressure, pCO_2 = 0.2 mm Hg; atmospheric pressure 560 mm Hg). The osmolarity was 312 ± 1 mOsm/l.

2.10. Statistical analysis

Results in the text are presented as average and standard deviation. The error bars in the graphs correspond to 95% confidence intervals. Distribution of data was assessed by Shapiro-Wilk or Kolmogorov-Smirnov tests, depending on sample sizes. Comparisons between groups were performed using analysis of variance for repeated measurements, or with the Friedman test with *post hoc* analysis with Dunnís test. Comparisons between groups with different flow rates and the presence of plasma or EGTA were performed with two-way analysis of variance and Bonferroni *post hoc* analysis. Bivariate correlation analysis was performed with Spearman coefficients. The significance level was set at $p < 0.05$. Statistical analysis was performed using GraphPad Prism (v6.0 package, demo version; GraphPad Software Inc., San Diego, CA).

3. Results

3.1. Cell viability and morphological changes

Cell viability calculated from hemoglobin release measurements did not decrease significantly after centrifugation with g-second values up to 9×10^5 g s, compared with non-treated negative controls (Fig. 2A). In the case of cells manipulated through the SPLITT channel, exposure to flow rates higher than 4.5 ml/min resulted in significantly decreased viability compared with negative controls (98.7 ± 0.6 and 99.9 ± 0.1, respectively; $p = 0.001$), but plasma supplementation reduced that effect ($p = 0.0001$) (Fig. 2B). After centrifugation, the morphological index increased progressively with centrifugal g-second values of $12 \times 10^5 g$ s and higher, compared to non-treated negative controls (Fig. 2C) (80.9 ± 10.0 and 17.0 ± 2.3 for centrifugation at $900 \times 105g$ s and negative controls, respectively; $p = 0.0001$). In SPLITT, exposure to flow rates from 1.5 to 10 ml/min resulted in significant increase in the morphological index compared with non-treated negative controls (53.9 ± 8.5 at 10 ml/min compared to 17.2 ± 2.4 in negative controls; $p = 0.0001$), though these changes were reduced in the presence of plasma ($p = 0.0001$) (Fig. 2D). The average cell diameter in non-treated negative controls was 8.38 ± 0.58 μm, and decreased significantly with exposure to centrifugation (7.45 ± 0.83 μm at a g-second value of $9 \times 10^5 g$ s) (Fig. 2E). Similarly, a significant reduction in average diameter was observed in cells exposed to incremental flow rates through the SPLITT channel, compared to negative controls (7.55 ± 0.67 μm in cells exposed to 10 ml/min; $p = 0.0001$). In the presence of autologous plasma, the diameter in negative control cells was significantly lower than in non-supplemented cells (7.81 ± 0.70 μm; $p = 0.0001$), and showed no significant change after exposure to flow through the SPLITT channel (Fig. 2F). Mean corpuscular hemoglobin concentration (MCHC) was 35.0 ± 0.8% in non-treated negative control cells and decreased to 30.4 ± 2.9% after centrifugation at $9 \times 10^5 g$ s ($p = 0.0021$) (Fig. 3G). Likewise, MCHC decreased significantly after the passage through the SPLITT channel to 30.2 ± 4.3% at 10.0 ml/min compared to negative controls ($p = 0.0032$) (Fig. 2H).

3.2. Hydrodynamic forces

Wall shear stress as an indicator of hydrodynamic stress depends on velocity and geometry. In the SPLITT channel, we observed that the maximum outlet shear stress values reflect speed changes caused by the reduced hydraulic diameter of the connector and by its angled orientation (Fig. 3A and B). In the lower outlet of the channel, the maximum velocities ranged from 0.05 to 0.4 m/s and shear stress was between 0.7 and 4.8 Pa at flow rates of 1.5 and 10 ml/min, respectively. In the centrifugation tube, however, the maximum wall shear stress zones reflect the cell trajectories during sedimentation to the bottom of the tube, as the cells collide with the tube walls. In the centrifuge tube, maximum velocities were between 10^{-6} and 10^{-4} m/s, and wall shear stresses ranged from 1.3 to 9.1×10^{-2} Pa (Fig. 4A). Moreover, two other indicators may serve to evaluate hydrodynamic stress: energy dissipation rate (EDR), which incorporates the velocity gradient in three; and pressure, which becomes important especially in centrifugation. In the SPLITT channel, the maximum EDR was 79,100 W/m^3 and

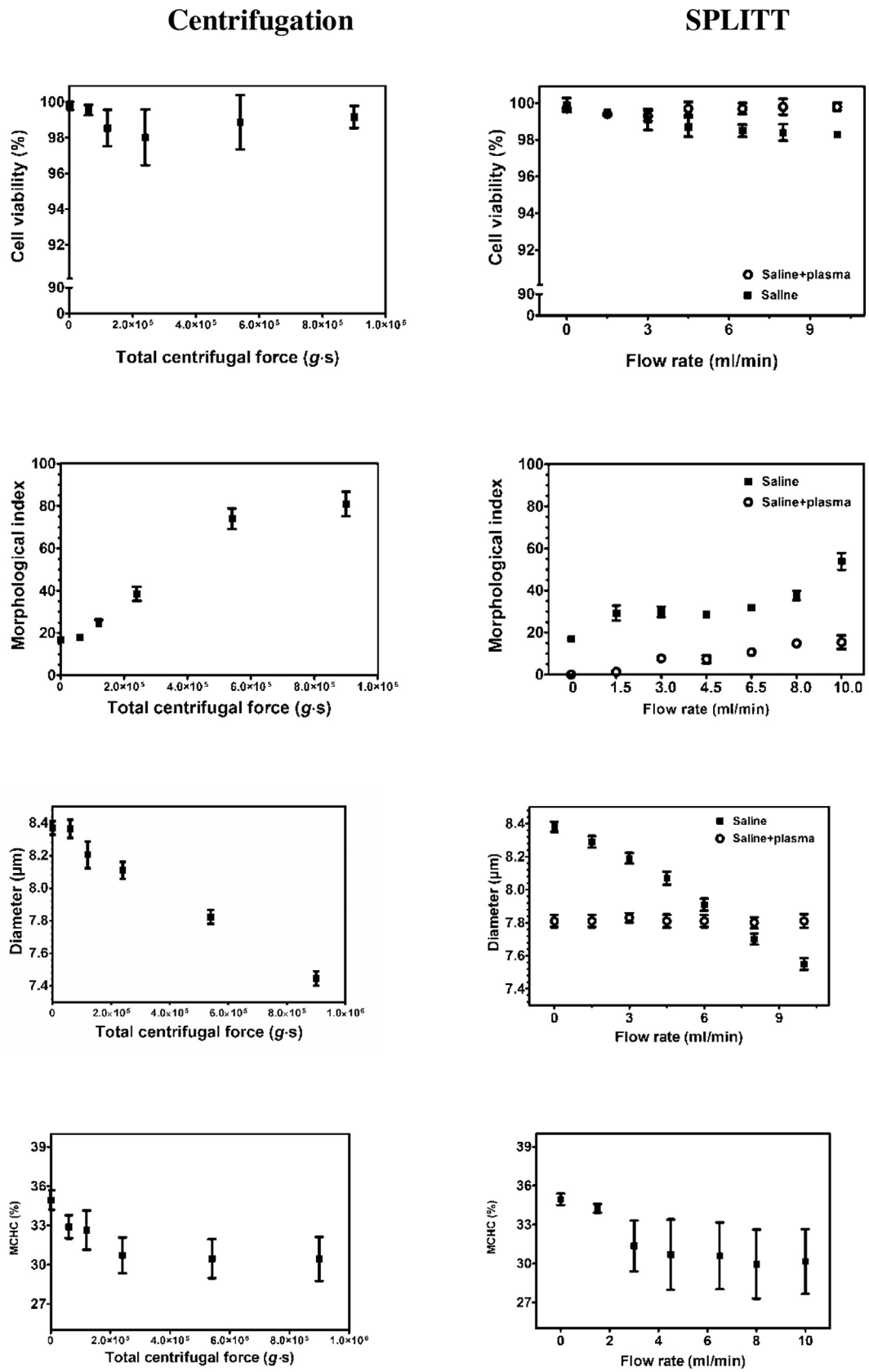

Fig. 2. Cell viability and morphological changes in red blood cells exposed to manipulation through the SPLITT channel or centrifugation. (A) Cell viability in cells exposed to centrifugation. (B) Cell viability of cells manipulated through the SPLITT channel. (C) Morphological index in red blood cells after centrifugation. (D) Morphological index in red blood cells manipulated through the SPLITT channel. (E) Diameter of red blood cells after centrifugation. (F) Diameter after manipulation through the SPLITT channel. (G) Mean corpuscular hemoglobin concentration of red blood cells after centrifugation. (H) Mean corpuscular hemoglobin concentration of red blood cells after a single pass through the SPLITT channel. In all cases, red blood cell dilution in saline were the same. When the flow rate or centrifugal force were zero, cells were not manipulated through any separation device (non-treated negative controls). Some assays in SPLITT were conducted in cells supplemented with autologous plasma (10% v/v) (open circles). Error bars correspond to 95% confidence intervals (n = 14).

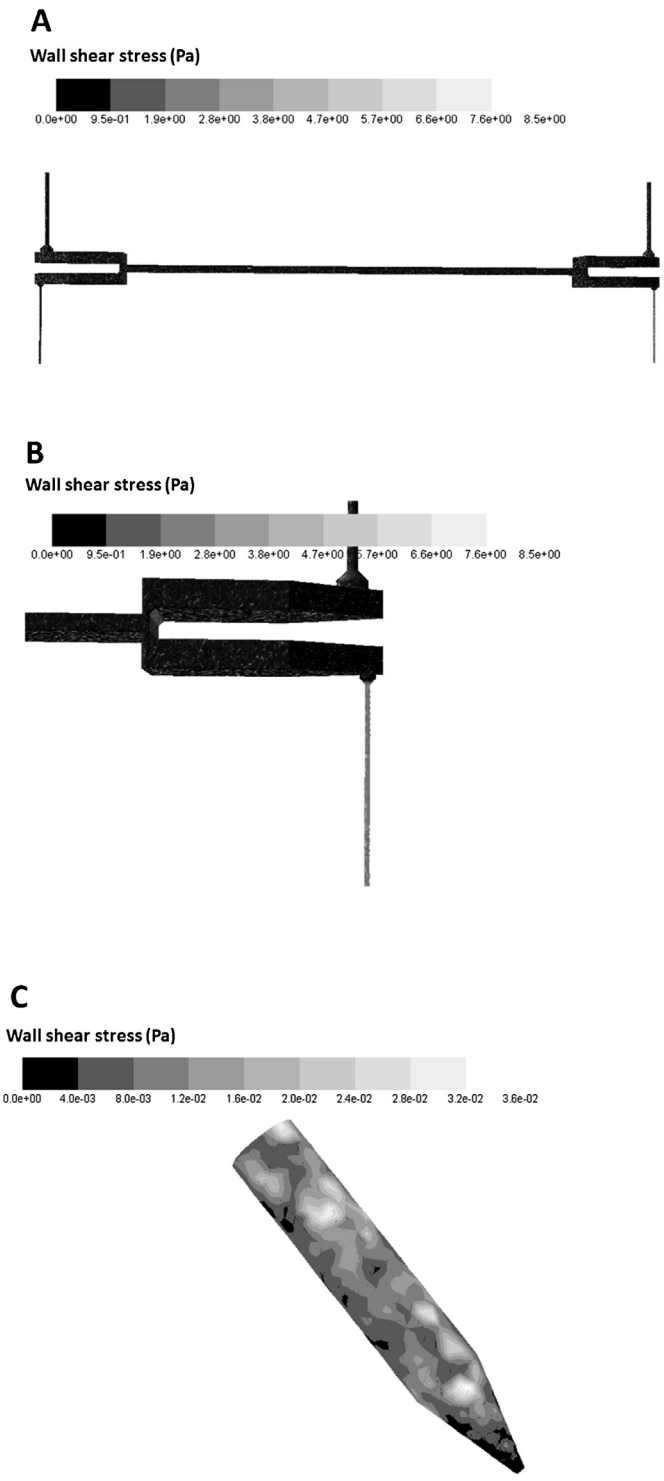

Fig. 3. Wall shear stress in the SPLITT channel and the centrifugation tube. (A) Wall shear stress in the SPLITT channel operated at a total flow rate of 10.0 ml/min with two inlets and one outlet (bottom). (B) Wall shear stress in the bottom outlet of the SPLITT channel when operated at 10.0 ml/min. (C) Wall shear stress in the centrifugation tube at 1500*g* ($9 \times 10^5 g$ s).

the pressure was 1100 Pa when operated at 10 ml/min. During centrifugation, the maximum EDR was 23 W/m^3 and the pressure was 1,032,450 Pa (10 atmospheres) at 1500*g* (Fig. 4B). To relate cell damage to the magnitude of hydrodynamic forces, a bivariate correlation analysis was performed. Maximum shear stress and maximum EDR showed a moderate correlation with lethal cell damage (hemolysis) (R = 0.495; $p = 0.502$). Maximum EDR correlated moderately with sublethal damage (morphological index) (R = 0.458; $p = 0.000$), but the correlation of sublethal damage with shear stress and pressure was poor (R = 0.396 and 0.296, respectively; $p = 0.000$).

3.3. Membrane potential

The average resting potential in the negative controls was -20.8 ± 3.0 mV, close to previously measured values with fluores-

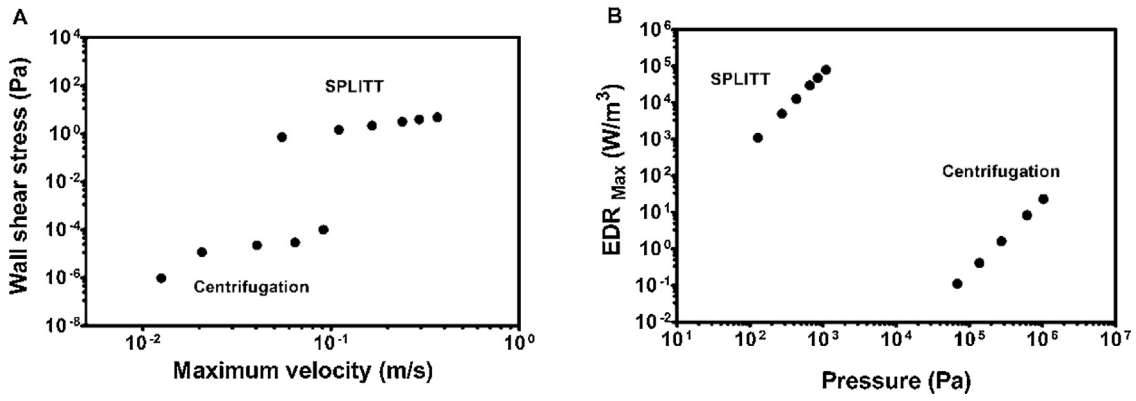

Fig. 4. Wall shear stress, velocity and maximum energy dissipation rate and pressure in the SPLITT channel operated at total flow rates between 1 and 10 ml/min, and in the centrifuge tube operated at 100–1500 *g*. (A) Wall shear stress and maximum velocity. (B) Maximum energy dissipation rate (EDR_{Max}) and pressure.

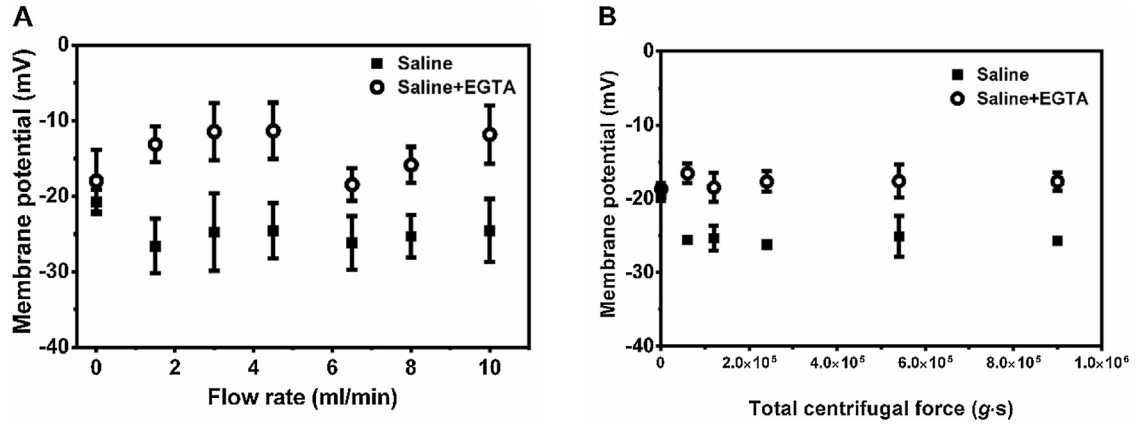

Fig. 5. Membrane potential in red blood cells exposed to hydrodynamic stress. (A) Cells manipulated through a SPLITT channel. (B) Cells after centrifugation. Cells suspended in saline solution (black squares). Cells suspended in saline solution with EGTA added (open circles). Results are shown as averages, and error bars correspond to 95% confidence interval (n = 14).

cent probes and with the patch clamp technique at pH 7.4 [20]. A significant hyperpolarization was observed after exposure to centrifugation (-25.7 ± 0.3 mV, $p < 0.05$) and after flow through the SPLITT channel (-26.6 ± 6.8 mV; $p = 0.01$). The addition of the calcium chelator EGTA resulted in complete inhibition of this effect in both cases ($p = 0.007$) (Fig. 5). Moreover, EGTA-treated cells showed no significant changes in the morphological index and diameter compared with the controls in saline with no EGTA (8.37 ± 0.54 μm after centrifugation at 1500*g*, and 8.36 ± 0.47 μm after exposure to 10 ml/min in the SPLITT channel; $p > 0.05$).

4. Discussion

This study evaluated the hydrodynamic damage on human red blood cells induced by SPLITT fractionation in gravitational mode or by simple centrifugation. Using parameters previously shown to separate blood cells by SPLITT fractionation (Fuh and Giddings, 1995) and centrifugal *g*-second values between 6 and $90 \times 10^4 gs$ in simple centrifugation [3,13] the cell viability was above 98%, which is acceptable. However, output fractions showed significant morphological changes, including appearance of abnormal shapes (echinocytes) and decreases in diameter and MCHC. The discoid shape of the red blood cell is critical for gas transport and is also a highly sensitive indicator of extracellular medium changes and mechanical stress [21]. This study shows that sample dilution in saline solution induced echinocytes, possibly due to temperature (20 ± 2 °C) which was lower than the physiological [17], and/or the absence of plasma and mechanical manipulation during pipetting [22]. However, even higher morphological index values were observed after SPLITT fractionation and centrifugation, which we directly related to flow rate and centrifugal acceleration, respectively. These findings suggest that appearance of echinocytes is a sensitive indicator of mechanical injury [16], triggered even by the low forces imposed by these separation systems. Echinocytosis may impact downstream processes and limit therapeutic effectiveness after transfusion, since these cells are more dense and fragile than discocytes and therefore can more easily undergo lysis [23,24].

Supplementation of autologous plasma protected against echinocyte formation both during sample dilution and after SPLITT. The protective effect of plasma and serum against mechanical stress has been attributed to physical mechanisms related to increased medium viscosity [25,26], decreased shear stress and turbulence [27], and prevention of cell-wall interactions [28]. In our experimental conditions and with the samples obtained from presumably healthy volunteers under fasting conditions, the final viscosity of the medium was not significantly different from the electrolytic solution alone (0.0013 Pa·s, compared to 0.0016 Pa•s with 10% plasma). Though viscosity-related effects can therefore be ruled out, it remains to determine whether the hydrodynamic damage seen in SPLITT channels is caused by cell-wall interactions which appear minimal in our experimental conditions [29], or whether it can be prevented by manipulating the surface material [30]. Beyond the possible physical effects of the plasma, biochemical mechanisms consistent with decreased membrane fluidity have been suggested to reduce shear sensitivity [31]. The relevance of erythrocyte membrane fluidity to morphological changes observed

after SPLITT fractionation, and the role of plasma supplementation, are to be determined.

It has been assumed that SPLITT has low impact on cells as the force and flow field used are low [4,12,32]. In agreement with these expectations, the hydrodynamic forces under our operating conditions can be classified as "sublethal" [33]. Contrary to the belief that SPLITT is innocuous, however, this study documents significant morphological and electrical changes in RBCs. Computational analysis of fluid dynamics shows that the zone of higher hydrodynamic stress in the SPLITT channel is the output connector. Although this is because the channel was operated with only one exit and not two, this is also due to the reduced hydraulic diameter and angled orientation of the connector. Reducing the cellular damage imposed by SPLITT could be achieved by supplementing with autologous plasma to increase the tolerance to mechanical stress [34], and increasing the diameter of the connectors and their orientation angle with respect to the channel to reduce hydrodynamic stress. Utilization of autologous plasma could be effective as cell protectant during cell separation, if used with otherwise frequently discarded plasma frozen within 24 h after phlebotomy or cryoprecipitate reduced plasma. With respect to the applicability of SPLITT fractionation to separation of large volumes of blood, it is noteworthy that, due to the high level of sample dilution, fractions obtained require a concentration step in order to achieve the high cell counts preferred in most laboratory applications. Additionally, due to the low flow rates used, processing larger sample volumes may require larger SPLITT devices.

Centrifugation in a Ficoll®-Paque density gradient is widely used to separate mononuclear and polymorphonuclear cells from whole blood, resulting in high purity fractions ($83.9 \pm 1.6\%$ of lymphocytes; $13.8 \pm 2.3\%$ of monocytes; and $96.4 \pm 1.0\%$ neutrophils) with cell viability greater than 98% [35]. After the separation process, the remaining RBCs in the densest fractions show decreased cell size, suggestive of cellular dehydration [36]. With respect to cell recovery and viability, the Ficoll-Paque technique appears to be inferior to others as e.g. Percoll density gradient centrifugation, immunomagnetic separation [37] and hypotonic lysis of red blood cells [38]. In addition, cells purified by this technique, although viable, may have functional impairments such as reduced cell proliferation [38] and attenuated cellular response as seen by depolarization after an activation stimulus (formyl-N-methionyl-leucyl-phenylalanine – FMLP), when compared with cells separated by other techniques [39]. We analyzed the hydrodynamic forces imposed to cells by simple centrifugation using centrifugal forces and times similar to that used in density centrifugation, cell washes and blood banks. Fluid dynamic analysis showed that although the velocity, shear stress and EDR were below the lytic damage zone, the hydrostatic pressure at the bottom of tube exceeded 10 atm, enough to produce significant cell damage [33,40,41]. After simple centrifugation, we observed morphological and electrical disturbances, indicating that the forces applied when washing cells and fractionating blood components may induce sublethal cell damage. It has been assumed that routine blood bank processing has low impact on cells, with a greater focus on so-called "storage lesions". Our data suggest the occurrence of a heretofore unnoticed "processing lesion". This suggests that the physical and biochemical deficits of blood components at the end of storage may be due to the cumulative effect of processing and cold storage.

In parallel to the appearance of abnormal erythrocyte forms, MCHC decreased by about 5%. Given that the observed cell death was less than 2%, an alternative explanation should be considered, for example, membrane blebbing and release of vesicles containing hemoglobin [42,43]. Indeed, spikes in echinocytes are part of an exosome release process from the plasma membrane [44]. It would be interesting to seek the presence of these organelles in the supernatant after hydrodynamic damage and determine their composition.

The observed decrease in cell diameter suggests that the hydrodynamic forces during separation via centrifugation and SPLITT activate mechanisms of regulatory cell volume decrease. It has been reported that CHO cells exposed to repetitive mechanical stress in a stirred bioreactor showed decreased cell diameter when EDR exceeded $6.4 \times 10^4\ W/m^3$ [7]. When a cell is transported by a fluid, the membrane experiences deformations which are dependent upon the movement of the fluid. In red blood cells, even small membrane deformations activate calcium-dependent efflux of potassium (Gardos channel, IK_1, KCa3.1) that result in hyperpolarization; and increased membrane potential promotes chloride and water leakage (cellular dehydration) [45]. Crenated and hyperpolarized erythrocytes appear as echinocytes [46]. The hyperpolarization observed after SPLITT fractionation and centrifugation would tend to support the occurrence of these processes. The inhibition of electrical and morphological changes in presence of EGTA suggests that extracellular calcium is essential not only in the activation of ion channels and cell volume regulation decrease but also in the generation of abnormal shapes in red blood cells [47].

Previous reports have stated that it is possible to obtain highly pure and viable fractions from whole blood using SPLITT fractionation [3]. Although several advantages have been attributed to SPLITT fractionation, such as low cost and the possibility of continuous separation without antibody labelling or separation matrix, in fact SPLITT requires highly diluted samples, which reduces throughput and requires a final concentration step to reach appropriate cell concentrations. Furthermore, although the low magnitude of the force fields used (low flow rates and $1\,g$) may lead to the assumption of low shear stress and preservation of cell integrity [4,12], the data presented here do not support these assumptions. Our results show that SPLITT fractionation is at least as damaging as simple centrifugation in terms of cell shape, size and membrane potential.

5. Conclusions

This study determined the effects of SPLITT fractionation on red blood cell morphology and membrane potential, compared with the effects of simple centrifugation. Besides the preservation of cell viability, both separation techniques induced a similar magnitude of sublethal hydrodynamic damage on red blood cells, observed as echinocyte formation, reduced MCHC and cell diameter, and calcium-dependent hyperpolarization. Our results do not support the position that SPLITT is harmless to cells, but show that this technique can be at least as harmful as simple centrifugation. Fluid dynamic analysis established that hemolytic and sublethal damage correlates with shear stress and maximum EDR. Within the SPLITT channel, the transport zone showed low stress, while the connectors showed the highest hydrodynamic forces, and an increase in diameter and angled orientation are suggested to decrease the potential for RBC damage. The addition of plasma to the carrier fluid used in SPLITT fractionation should also be considered, since this was protective against morphological damage and lysis. Industrial cell lines employed to produce substances with biological activity are much more robust in terms of resistance to hydrodynamic cell damage than human red blood cells. Sublethal damage is, therefore, much more difficult to detect [7]. Use of measurements of membrane potential and cell diameter could provide a new, reliable and convenient basis for evaluation of hydrodynamic effects on different cell models, allowing identification of optimal operating conditions on different scales.

Acknowledgments

This study was supported by the research division of Universidad Nacional de Colombia DIB, Bogotá, postgraduate thesis support program Hermes #14235; and grants from COLCIENCIAS, Biotechnology program nos. 222840820479 and 222856933541; and ECOS-Nord – COLCIENCIAS program C12PS01, 0385-2011. We acknowledge Dr. Michael Delay for critical review of the manuscript.

References

[1] S.O. Sowemimo-Coker, Red blood cell hemolysis during processing, Transfus. Med. Rev. 16 (2002) 46–60.
[2] J.C. Giddings, A system based on split-flow lateral-transport thin (SPLITT) separation cells for rapid and continuous particle fractionation, Sep. Sci. Technol. 20 (1985) 749–768.
[3] C.B. Fuh, J.C. Giddings, Isolation of human blood cells platelets, and plasma proteins by centrifugal SPLITT fractionation, Biotechnol. Prog. 11 (1995) 14–20.
[4] M.-A. Benincasa, L.R. Moore, P.S. Williams, E. Poptic, F. Carpino, M. Zborowski, Cell sorting by one gravity SPLITT fractionation, Anal. Chem. 77 (2005) 5294–5301.
[5] Z. Zhang, Y. Chisti, M. Moo-young, Effects of the hydrodynamic environment and shear protectants on survival of erythrocytes in suspension, J. Biotechnol. 43 (1995) 33–40.
[6] Y. Chisti, Hydrodynamic damage to animal cells, Crit. Rev. Biotechnol. 21 (2001) 67–110.
[7] R. Godoy-Silva, J.J. Chalmers, S.A. Casnocha, L.A. Bass, N. Ma, Physiological responses of CHO cells to repetitive hydrodynamic stress, Biotechnol. Bioeng. 103 (2009) 1103–1117.
[8] M. Bluestein, L. Mockros, Hemolytic effects of energy dissipation in flowing blood, Med. Biol. Eng. Comput. 7 (1969) 1–16.
[9] M. Moo-Young, Y. Chisti, Considerations for designing bioreactors for Shear-Sensitive culture, Nat. Biotechnol. 6 (1988) 1291–1296.
[10] D. Sakota, R. Sakamoto, N. Yokoyama, M. Kobayashi, S. Takatani, Glucose depletion enhances sensitivity to shear stress-induced mechanical damage in red blood cells by rotary blood pumps, Artif. Organs 33 (2009) 733–739.
[11] D. Sakota, R. Sakamoto, H. Sobajima, N. Yokoyama, S. Waguri, K. Ohuchi, et al., Mechanical damage of red blood cells by rotary blood pumps: selective destruction of aged red blood cells and subhemolytic trauma, Artif. Organs 32 (2008) 785–791.
[12] M. Hoyos, Separación hidrodinámica de macromoléculas, partículas y células, Acta Biológica Colomb. 8 (2003) 11–24.
[13] American Association of Blood Banks, Standards for Blood Banks and Transfusion Services, 28th edition, American Association of Blood Banks, Bethesda, MD, 2012.
[14] V. Han, K. Serrano, D.V. Devine, A comparative study of common techniques used to measure haemolysis in stored red cell concentrates, Vox Sang. 98 (2010) 116–123.
[15] J. Sikora, S.N. Orlov, K. Furuya, R. Grygorczyk, Hemolysis is a primary ATP-release mechanism in human erythrocytes, Blood 124 (2014) 2150–2157.
[16] K.L. Black, R.D. Jones, The discocyte-Echinocyte transformation as an index of human red cell trauma, Ohio J. Sci. 76 (1976) 225–230.
[17] G. Brecher, M. Bessis, Present status of spiculed red cells and their relationship to the discocyte-Echinocyte transformation: a critical review, Blood 40 (1972) 333–344.
[18] M. Mollet, R. Godoy-Silva, C. Berdugo, J.J. Chalmers, Acute hydrodynamic forces and apoptosis: a complex question, Biotechnol. Bioeng. 98 (2007) 772–788.
[19] T. Klapperstück, D. Glanz, M. Klapperstück, J. Wohlrab, Methodological aspects of measuring absolute values of membrane potential in human cells by flow cytometry, Cytometry A 79A (2011) 1023.
[20] J.F. Hoffman, P.C. Laris, Determination of membrane potentials in human and Amphiuma red blood cells by means of a fluorescent probe, J. Physiol 239 (1974) 519–552.
[21] S. Svetina, Red blood cell shape and deformability in the context of the functional evolution of its membrane structure, Cell. Mol. Biol. Lett. 17 (2012) 171–181.
[22] G.M. Artmann, K.L. Sung, T. Horn, D. Whittemore, G. Norwich, S. Chien, Micropipette aspiration of human erythrocytes induces echinocytes via membrane phospholipid translocation, Biophys. J. 72 (1997) 1434–1441.
[23] W.H. Reinhart, S. Chien, Red cell rheology in stomatocyte-echinocyte transformation: roles of cell geometry and cell shape, Blood 67 (1986) 1110–1118.
[24] O.K. Baskurt, H.J. Meiselman, Red blood cell mechanical stability test, Clin. Hemorheol. Microcirc. 55 (2013) 55–62.
[25] M.S. Croughan, E.S. Sayre, D.I.C. Wang, Viscous reduction of turbulent damage in animal cell culture, Biotechnol. Bioeng. 33 (1989) 862–872.
[26] A. McQueen, J.E. Bailey, Influence of serum level cell line, flow type and viscosity on flow-induced lysis of suspended mammalian cells, Biotechnol. Lett. 11 (1989) 531–536.
[27] M. Hulscher, J. Pauli, U. Onken, Influence of protein concentration on mechanical cell damage and fluidoynamics in airlift reactors for mammalian cell culture, Food Biotechnol. 4 (1990) 157–166.
[28] R.M. Hochmuth, N. Mohandas, E.E. Spaeth, J.R. Williamson, P.L. Blackshear, D.W. Johnson, Surface adhesion, deformation and detachment at low shear of red cells and white cells, Trans. Am. Soc. Artif. Intern. Organs 18 (1972) 325–334.
[29] I.C. Navarrete, M.M. Camacho, M. Hoyos, Modelo físico de los parámetros y efectos hidrodinámicos involucrados en una separación óptima de células usando una técnica campo-flujo (S-SPLITT), in: Tesis De Maestría En Ciencias – Física, Universidad Nacional de Colombia, 2013.
[30] T. Chianéa, P.J. Cardot, E. Assidjo, J. Monteil, I. Clarot, P. Krausz, Field- and flow-dependent trapping of red blood cells on polycarbonate accumulation wall in sedimentation field-flow fractionation, J. Chromatogr. B Biomed. Sci. App. 734 (1999) 91–99.
[31] O.T. Ramirez, R. Mutharasan, Effect of serum on the plasma membrane fluidity of hybridomas: an insight into its shear protective mechanism, Biotechnol. Prog. 8 (1992) 40–50.
[32] M. Hoyos, A. Niño, M. Camargo, J.C. Díaz, S. León, M. Camacho, Separation of Leishmania-infected macrophages by step-SPLITT fractionation, J. Chromatogr. B Analyt. Technol. Biomed. Life. Sci. 877 (2009) 3712–3718.
[33] N. Ma, K.W. Koelling, J.J. Chalmers, Fabrication and use of a transient contractional flow device to quantify the sensitivity of mammalian and insect cells to hydrodynamic forces, Biotechnol. Bioeng. 80 (2002) 428–437.
[34] M.V. Kameneva, J.F. Antaki, K.K. Yeleswarapu, M.J. Watach, B.P. Griffith, H.S. Borovetz, Plasma protective effect on red blood cells exposed to mechanical stress, ASAIO J. 43 (1997) M571–575.
[35] A. Ferrante, Y.H. Thong, A rapid one-step procedure for purification of mononuclear and polymorphonuclear leukocytes from human blood using a modification of the Hypaque-Ficoll technique, J. Immunol. Methods 24 (1978) 389–393.
[36] L.P. Bignold, A. Ferrante, Mechanism of separation of polymorphonuclear leukocytes from whole blood by the one-step Hypaque-Ficoll method, J. Immunol. Methods 96 (1987) 29–33.
[37] C. Pösel, K. Möller, W. Fröhlich, I. Schulz, J. Boltze, D.-C. Wagner, Density gradient centrifugation compromises bone marrow mononuclear cell yield, PLoS One 7 (2012) e50293.
[38] C.K. Keong, V.D.V. Nadarajah, T.J. Lee, Development of a purification method of pure primary lymphocytes for cell viability assays, Malays. J. Med. Sci. 14 (2007) 38–45.
[39] R.L. Berkow, S.J. Weisman, D. Tzeng, R.A. Haak, F.W. Kleinhans, S. Barefoot, et al., Comparative responses of human polymorphonuclear leukocytes obtained by counterflow centrifugal elutriation and Ficoll-Hypaque density centrifugation. II. Membrane potential changes membrane receptor analysis, membrane fluidity, and analysis of the effects of the preparative techniques, J. Lab. Clin. Med. 104 (1984) 698–710.
[40] P.L. Blackshear, F.D. Dorman, J.H. Steinbach, Some mechanical effects that influence hemolysis, ASAIO J. 11 (1965) 112–117.
[41] L.B. Leverett, J.D. Hellums, C.P. Alfrey, E.C. Lynch, Red blood cell damage by shear stress, Biophys. J. 12 (1972) 257–273.
[42] F.A. Willekens, B. Roerdinkholder-Stoelwinder, Y. Groenen-Döpp, H. Bos, l Bosman, A. Bos, et al., Hemoglobin loss from erythrocytes in vivo results from spleen-facilitated vesiculation, Blood 101 (2003) 747–751.
[43] F. Willekens, J.M. Werre, Y. Groenen-Döpp, B. Roerdinkholder-Stoelwinder, B. De Pauw, G. Bosman, Erythrocyte vesiculation: a self-protective mechanism? Br. J. Haematol. 141 (2008) 549–556.
[44] J.-D. Tissot, G. Canellini, O. Rubin, A. Angelillo-Scherrer, J. Delobel, M. Prudent, et al., Blood microvesicles: from proteomics to physiology, Transl. Proteomics 1 (2013) 38–52.
[45] A. Dyrda, U. Cytlak, A. Ciuraszkiewicz, A. Lipinska, A. Cueff, G. Bouyer, et al., Local membrane deformations activate Ca2+-Dependent K+ and anionic currents in intact human red blood cells, PLoS One 5 (2010) 1–14.
[46] M.M. Gedde, W.H. Huestis, Membrane potential and human erythrocyte shape, Biophys. J. 72 (1997) 1220–1233.
[47] S. Lin, E. Yang, W.H. Huestis, Relationship of phospholipid distribution to shape change in Ca(2+)-crenated and recovered human erythrocytes, Biochemistry 33 (1994) 7337–7344.